



## Abstract

Probability estimates of the future change of extreme precipitation events are usually based on a limited number of available Global Climate Model (GCM) or Regional Climate Model (RCM) simulations. Since floods are related to heavy precipitation events, this restricts the assessment of flood risks. In this study a relatively simple method has been developed to get a better picture of the range of changes in extreme precipitation events. Five bias corrected RCM simulations of the 1971–2100 climate for a single greenhouse gas emission scenario (A1B SRES) were available for the Rhine basin. To increase the size of this five-member RCM ensemble, 13 additional GCM simulations were analysed. The climate responses of the GCMs are used to modify an observed (1961–1995) precipitation/temperature time series with an advanced delta change approach. Changes in the temporal means and variability are taken into account. Time series resampling was applied to extend 35-yr GCM and RCM time-slices to 3000-yr series to estimate extreme precipitation with return periods up to 1000 yr. It is found that the range of future change of extreme precipitation across the five-member RCM ensemble is similar to results from the 13-member GCM ensemble. For the RCM ensemble, the time series modification procedure also resulted in a similar climate response compared to the signal deduced from the direct model simulations. The changes from the individual RCM simulations, however, systematically differ from those of the driving GCMs, especially for long return periods.

## 1 Introduction

Heavy precipitation events are of importance since they are a major cause of floods, which can have large impacts on society. Based on a wide range of observational and Regional Climate Model (RCM) studies, changes in greenhouse gas concentrations are expected to affect the frequency and magnitude of extreme precipitation. These studies show an intensification of precipitation extremes over most of Europe (Beniston

HESSD

9, 6533–6568, 2012

## Future changes in extreme precipitation in the Rhine basin

S. C. van Pelt et al.

Title Page

Abstract

Introduction

Conclusions

References

Tables

Figures

◀

▶

◀

▶

Back

Close

Full Screen / Esc

Printer-friendly Version

Interactive Discussion



et al., 2007; Buonomo et al., 2007; Fowler and Ekström, 2009; Frei et al., 2006; Hanel and Buishand, 2011; Kyselý and Beranová, 2009; Kyselý et al., 2011; Nikulin et al., 2011). The projections of changes in the precipitation extremes are sensitive to the choice of RCMs, the driving Global Climate Model (GCM) and the emission scenario.

5 Credible high-resolution climate scenarios for impact studies require an ensemble of RCM simulations driven by multiple GCMs (Fowler et al., 2007; Bernstein et al., 2007). Ideally such ensembles should represent the full range of natural variability and model uncertainty. In practice, however, they are assembled on an opportunity basis, and often the size of the ensembles is restricted by limited resources (Kendon et al., 2010).

10 In this study we used bias corrected output of five RCM simulations available through the Rheinblick2050 project (Görgen et al., 2010), where a comprehensive ensemble of hydrological simulations driven by the output of RCMs was used to analyse future changes in the Rhine discharge regime. The five RCMs were driven by GCMs that were all forced with the A1B SRES emission scenario. It is of interest to assess to what  
15 degree the results based on such a small sample size underestimate the uncertainty associated with the model error and natural variability. RCMs can resolve small scale features, but can still contain large biases, partly inherited from the driving GCMs. The five-member RCM ensemble from the Rheinblick2050 project was extended with an ensemble of 13 GCM simulations to get a better picture of the uncertainty induced by  
20 the GCM ensemble. This uncertainty is believed to exceed the uncertainty arising from the choice of downscaling techniques and emission scenarios (Graham et al., 2007; Menzel et al., 2006; Prudhomme and Davies, 2009; Rowell, 2006; Wilby and Harris, 2006). Also the GCM ensemble was driven by the A1B emission scenario. Since high resolution RCM simulations from all these 13 GCM simulations were not available we  
25 followed a pragmatic approach by post-processing the GCM outputs, using “change factors” (Diaz-Nieto and Wilby, 2005; Arnell and Reynard, 1996), also referred to as the *delta change approach* (Prudhomme et al., 2002; Te Linde et al., 2010; Lenderink et al., 2007).

**Future changes in extreme precipitation in the Rhine basin**

S. C. van Pelt et al.

Title Page

Abstract

Introduction

Conclusions

References

Tables

Figures



Back

Close

Full Screen / Esc

Printer-friendly Version

Interactive Discussion





2200 m<sup>3</sup> s<sup>-1</sup>. The estimated 1250-yr return level at this site, which is used as design discharge in the Netherlands, is 16 000 m<sup>3</sup> s<sup>-1</sup>.

The climate in the Rhine basin is determined by its location in a West-European zone of temperate climatic conditions with frequent synoptic weather changes. From the northwest to the east and southeast, the maritime climate gradually changes into a more continental climate. Precipitation occurs all year round; maximum annual precipitation in the mountains can be as high as 3000 mm, whilst in valleys at the lee side annual precipitation is only 600 mm. Spatially averaged annual precipitation sums between 1901 and 2000 (Belz et al., 2007) point towards a slight increase in different sub-regions against a fairly uniform background decadal scale variability. Thereby the increase of precipitation during the hydrological winter is more pronounced.

## 2.2 RCM and GCM data set

In Table 1 an overview is given of the daily RCM and GCM precipitation and temperature output considered in this study. In the Rheinblick2050 project (Görgen et al., 2010) the RCM simulations were used as input of the hydrological model (HBV) for the Rhine basin to study the impact of climate change on the discharge in this river basin. We have selected five out of the six RCM simulations used in the Rheinblick2050 project for extreme river flows. The ARPEGE-HIRHAM simulation was left out of the analysis because its complex reduced grid structure did not allow a straightforward interpolation to a common grid. With the exception of the REMO\_10 simulation, the RCM data were obtained from the archive of the ENSEMBLES project (Van der Linden and Mitchell, 2009). Model specific bias corrections were derived by comparing the RCM control simulations with a high resolution precipitation and temperature data set.

The additional GCM data were obtained from the Coupled Model Intercomparison Project Phase 3 (CMIP3) archive (Meehl et al., 2007). All GCM simulations used are driven by the commonly available A1B emission scenario. The GCM output is interpolated to a common 2° lon by 2.5° lat grid. The Rhine basin is covered by eight grid cells

## Future changes in extreme precipitation in the Rhine basin

S. C. van Pelt et al.

Title Page

Abstract

Introduction

Conclusions

References

Tables

Figures

◀

▶

◀

▶

Back

Close

Full Screen / Esc

Printer-friendly Version

Interactive Discussion



(see Fig. 1). For all GCMs a control run period of 35 yr (1961–1995) and a scenario run period of 20 yr (2081–2100) was used.

## 2.3 The precipitation and temperature observations

Observations of precipitation and temperature for the Rhine basin are available from the International Commission for the Hydrology of the Rhine basin (CHR). The so-called CHR-OBS dataset (Sprokkereef, 2001) contains area-averaged daily precipitation and temperature for 134 sub-basins of the Rhine basin that were defined for hydrological simulations with the HBV (Hydrologiska Bryåns Vattenblansavdelning) model. CHR-OBS data were available for the period 1961–1995. A newer and longer precipitation data set has become available recently (Photiadou et al., 2011) but this was not used in this study. In a companion study, the HBV model is used to analyse and interpret the results described in this paper in terms of changes of flood risk (Ward et al., 2012).

## 3 Methodology

### 3.1 Time series transformation

#### 3.1.1 Nonlinear delta method for precipitation

An advanced delta method is used to transform the CHR observations into a time series that is representative of future conditions consistent with the GCM climate change signal. The delta method makes use of “change factors”, and is therefore also referred to as the *delta change approach*. The most simple form of the delta method (sometimes referred to as the “classical delta method”), only considers changes in the mean. The change in the mean may vary seasonally throughout the year or spatially. When coupling with impact models is required (e.g. with a hydrological model), delta methods have a practical advantage that an (observed) reference time series at the temporal and

## Future changes in extreme precipitation in the Rhine basin

S. C. van Pelt et al.

Title Page

Abstract

Introduction

Conclusions

References

Tables

Figures

◀

▶

◀

▶

Back

Close

Full Screen / Esc

Printer-friendly Version

Interactive Discussion



spatial scale of interest can be used to represent the current climate. The assumption that one has to make is that changes at the (large) scale of the climate model (GCM) can be directly applied to the (local) scale of the time series.

In this study, a more advanced delta method is introduced, that not only takes changes in the mean into account but also the changes in the extremes. Again these changes can vary seasonally and spatially. Rather than a proportional adjustment of observed precipitation, a non-linear transformation is applied (see also Fig. 1 for a graphical summary of the complete procedure):

$$P^* = aP^b \quad (1)$$

where  $P$  and  $P^*$  represent the observed and (transformed) future precipitation, respectively, and  $a$  and  $b$  are the transformation coefficients ( $a, b > 0$ ). This type of transformation was first applied for bias correction of precipitation in the Meuse basin by Leander and Buishand (2007). Several studies have indicated that extreme discharges in the lower part of the Rhine generally result from extreme multi-day precipitation amounts in the river basin. For instance, during the December 1993 and January 1995 floods precipitation was extreme over a 10-day period (Disse and Engel, 2001; Ulbrich and Fink, 1995). Therefore the future change in (extreme) multi-day precipitation is more relevant than the change in (extreme) daily precipitation. In this study Eq. (1) is applied to non-overlapping 5-day sums (73 5-day periods in a calendar year of 365 days). The 5-day time step recognizes the relevance of multi-day precipitation sums, but yet is small enough to be linked with daily precipitation as well.

The coefficients  $a$  and  $b$  are derived from the 60% quantile ( $P_{60}$ ) and the 90% quantile ( $P_{90}$ ) of the 5-day precipitation sums and the (future) changes therein. Sample quantiles based on the ordered non-overlapping 5-day precipitation amounts were used as estimates of  $P_{60}$  and  $P_{90}$ .  $P_{60}$  is considered because this quantile is generally closer to the mean than the median value ( $P_{50}$ ) owing to the positively skewed probability distribution of the 5-day precipitation amounts.  $P_{90}$  (which is exceeded on average once in ten 5-day periods) is in the range of the seasonal maximum 5-day precipitation

## Future changes in extreme precipitation in the Rhine basin

S. C. van Pelt et al.

[Title Page](#)[Abstract](#)[Introduction](#)[Conclusions](#)[References](#)[Tables](#)[Figures](#)[Back](#)[Close](#)[Full Screen / Esc](#)[Printer-friendly Version](#)[Interactive Discussion](#)

amounts (see Appendix A). Since the transformation given by Eq. (1) represents a monotonic increase, the quantiles of the transformed 5-day precipitation sums are simply obtained by applying the same transformation to the quantiles of the observed 5-day precipitation:

$$5 \quad P_{60}^* = a(P_{60})^b \quad (2)$$

$$P_{90}^* = a(P_{90})^b \quad (3)$$

From these two equations, first  $b$  is solved by eliminating  $a$  (Leander and Buishand, 2007):

$$10 \quad b = \frac{\log(P_{90}^*/P_{60}^*)}{\log(P_{90}/P_{60})} \quad (4)$$

Once  $b$  is determined,  $a$  is obtained by substituting  $b$  into Eq. (2):

$$a = P_{60}^*/(P_{60})^b \quad (5)$$

If there is no bias in  $P_{60}^C$  and  $P_{90}^C$  in the GCM control simulation compared to the observations, the quantiles  $P_{60}^C$  and  $P_{90}^C$  can be substituted for  $P_{60}$  and  $P_{90}$  in Eqs. (4) and  
 15 (5), and the quantiles  $P_{60}^F$  and  $P_{90}^F$  in the future climate for  $P_{60}^*$  and  $P_{90}^*$ . However, if  $P_{60}$  and  $P_{90}$  are biased, this method results in a transformation that does not reproduce the relative changes in these quantiles. In order to ensure that the relative changes of  $P_{60}$  and  $P_{90}$  in the transformed series correspond to the relative changes of these quantiles in the GCM simulation, the following bias-correction factors are introduced:

$$20 \quad g_1 = P_{60}^O/P_{60}^C \quad (6)$$

and

## Future changes in extreme precipitation in the Rhine basin

S. C. van Pelt et al.

Title Page

Abstract

Introduction

Conclusions

References

Tables

Figures

◀

▶

◀

▶

Back

Close

Full Screen / Esc

Printer-friendly Version

Interactive Discussion



$$g_2 = P_{90}^O / P_{90}^C \quad (7)$$

where the superscript “C” again refers to the GCM control climate and “O” refers to observed (reference) data. These corrections are applied to  $P_{60}^C$  and  $P_{90}^C$  as well as  $P_{60}^F$  and  $P_{90}^F$ . The coefficients  $a$  and  $b$  then become:

$$b = \frac{\log\{g_2 \cdot P_{90}^F / (g_1 \cdot P_{60}^F)\}}{\log\{g_2 \cdot P_{90}^C / (g_1 \cdot P_{60}^C)\}} \quad (8)$$

$$a = P_{60}^F / (P_{60}^C)^b \cdot g_1^{1-b} \quad (9)$$

Note that the classical delta change method is obtained by assuming that the GCM responses in the 60 %- and 90 %-quantiles are equal:

$$P_{90}^F / P_{90}^C = P_{60}^F / P_{60}^C \quad (10)$$

leading to  $b = 1$  and  $a = P_{60}^F / P_{60}^C$  and, therefore Eq. (1) reduces to  $P^* = aP$ .

Equation (1) is applied to the observed values for which  $P \leq P_{90}$ . For larger  $P$  this equation may result in unrealistically high precipitation values when  $b > 1$ . The transformation (1) is also not flexible enough to reproduce the changes in the extremes adequately. This can be improved by separately addressing the change in the excesses,  $E = P - P_{90}$ , i.e. the events exceeding  $P_{90}$ . The mean excesses for the control and future period are defined as:

$$\overline{E^C} = \frac{\sum E^C}{n^C} \quad \text{and} \quad \overline{E^F} = \frac{\sum E^F}{n^F} \quad (10)$$

where  $n^C$  and  $n^F$  are the numbers of 5-day periods during which the 90 % quantile is exceeded in the control and future run, respectively. The size of the mean excess is

## Future changes in extreme precipitation in the Rhine basin

S. C. van Pelt et al.

Title Page

Abstract

Introduction

Conclusions

References

Tables

Figures

◀

▶

◀

▶

Back

Close

Full Screen / Esc

Printer-friendly Version

Interactive Discussion



closely related to the slope of an extreme-value plot of the seasonal maximum 5-day precipitation amounts (see Appendix A).

To ensure that the transformation reproduces the change in the mean excess, Eq. (1) is modified as:

$$P^* = \overline{E^F} / \overline{E^C} \cdot (P - P_{90}^O) + a(P_{90}^O)^b \text{ for } P > P_{90}^O \quad (11)$$

Effectively the excess scales linearly with the factor  $\overline{E^F} / \overline{E^C}$ . This linear scaling of the excess avoids unrealistically high precipitation amounts.

In principle the coefficients  $a$  and  $b$  and the change in the mean excesses  $\overline{E^F} / \overline{E^C}$  may vary seasonally and spatially. To reduce sampling variability in the transformation coefficients we chose to use smoothed, but distinct values of  $a$ ,  $b$  and  $\overline{E^F} / \overline{E^C}$  for each calendar month. First, the quantiles  $P_{60}$  and  $P_{90}$  are estimated for each calendar month using six 5-day periods for the calendar months January to November and seven 5-day periods for December. These monthly estimates of  $P_{60}$  and  $P_{90}$  are subsequently smoothed by using a weight of  $1/2$  placed on the calendar month of interest and weights of  $1/4$  on the preceding and following calendar months. Taking longer time windows for smoothing of the annual cycle did not affect our results markedly. The mean excesses  $\overline{E^C}$  and  $\overline{E^F}$  are smoothed over time similarly. The temporally smoothed estimates of  $P_{60}$  and  $P_{90}$  are used in Eq. (8) to obtain a temporally smoothed value of  $b$  for each calendar month and for each grid cell in the basin. To reduce sampling variability further, the median value of  $b$  over the eight grid cells for each calendar month is used for all grid cells in the basin. Analogously, the median of  $\overline{E^F} / \overline{E^C}$  over the eight grid cells is taken for each calendar month. The coefficient  $a$  finally varies spatially (a distinct value for each grid cell in the basin) and is obtained by using the temporally smoothed  $P_{60}$  and the spatially uniform value of  $b$  in Eq. (9).

Here daily precipitation amounts for the 134 HBV sub basins in the Rhine basin for the period 1961–1995 are used as the baseline time series. Equations (1) and (11), however, apply to the area-average precipitation over a GCM grid cell. The precipitation

**Future changes in extreme precipitation in the Rhine basin**

S. C. van Pelt et al.

Title Page

Abstract

Introduction

Conclusions

References

Tables

Figures



Back

Close

Full Screen / Esc

Printer-friendly Version

Interactive Discussion



amounts for the HBV sub basins were therefore aggregated to grid cell values by taking an area-weighted average of the sub-basins lying in the respective grid cell. After the transformation using Eqs. (1) and (11) the final step involves the disaggregation of the transformed 5-day precipitation values at the GCM grid cell into daily precipitation at the sub basin scale. For this a change factor  $R$  was defined for each grid cell and 5-day period as:

$$R = P^* / P \quad (12)$$

Each daily observation in a sub-basin allocated to a given GCM grid cell is transformed according to the corresponding value of  $R$ . Thus, the daily observations in a 5-day sequence obtain the same relative change. The method ensures that the change in the temporally and spatially aggregated daily precipitation of the sub-basins corresponds to the change in the 5-day precipitation over the grid cell. The non-linear nature of Eqs. (1) and (11) generally results in different change factors for days in distinct 5-day intervals. The result is a future time series of daily precipitation on sub-basin level.

### 3.1.2 Motivation for temporal and spatial smoothing and bias correction

Temporal and spatial smoothing was applied to reduce the influence of sampling noise on the estimated climate change signal. Spatial variation of  $b$  and  $\overline{E^F} / \overline{E^C}$  was ignored. The need for temporal and spatial smoothing is shown in Fig. 2 for two GCM simulations. The changes from the model output were used to transform the observed data, both with and without temporally and spatially smoothed coefficients in Eqs. (1) and (11). The figure gives the relative changes of the return levels of 10-day precipitation for the winter-half year (October–March) as a function of return period. The changes are shown for each grid cell of the Rhine basin separately. Similar figures were made for all other GCM simulations. For the transformed data based on the CGCM3.1T63 simulation (left of Fig. 2) an unrealistically large increase for return periods  $>10$  yr is found at grid cell 4 when no smoothing is applied. The results for the ECHAM5r1 simulation

## Future changes in extreme precipitation in the Rhine basin

S. C. van Pelt et al.

Title Page

Abstract

Introduction

Conclusions

References

Tables

Figures

◀

▶

◀

▶

Back

Close

Full Screen / Esc

Printer-friendly Version

Interactive Discussion



(right) are characteristic for most other GCM simulations. The spread of the relative changes strongly increases with increasing return period when temporal and spatial smoothing are not applied. Smoothing also improves the correspondence between the changes in the mean precipitation and the mean 10-day maximum basin-average precipitation from the transformed time series and the changes in these properties from the climate model output (not shown).

The sensitivity to the bias correction of the transformation coefficients was tested by comparing the relative changes in the transformed data to the changes in the GCM output taking either  $g_1$  and  $g_2$  as specified using Eqs. (6) and (7) or  $g_1 = g_2 = 1$ , i.e. without bias correction. Figure 3 shows the results for the maximum basin-average precipitation for the summer half-year (April–September) and the winter half-year. For summer the bias correction on both  $P_{60}$  and  $P_{90}$  leads to the best correspondence between the transformed time series and the direct GCM simulations. For winter the bias corrections only play a minor role.

### 3.1.3 Delta method for temperature

The observed daily temperature is transformed for each sub-basin taking into account the changes in the mean and standard deviation of the daily temperatures from the GCM simulation:

$$T^* = \frac{\sigma^F}{\sigma^C} (T - \overline{T^O}) + \overline{T^O} + \overline{T^F} - \overline{T^C} \quad (13)$$

where  $T$  and  $T^*$  represent the observed and transformed daily temperature, respectively.  $\overline{T^O}$  is the mean of the observed daily temperature.  $\overline{T^F}$ ,  $\sigma^F$  are the mean and standard deviation of the future daily temperature series and  $\overline{T^C}$ ,  $\sigma^C$  are the mean and standard deviation of the control daily temperature series. As for precipitation, the mean and standard deviation are determined for each month and for each grid cell. The standard deviation is smoothed over time using the same 3-month moving average filter as for the precipitation statistics.

## Future changes in extreme precipitation in the Rhine basin

S. C. van Pelt et al.

Title Page

Abstract

Introduction

Conclusions

References

Tables

Figures

◀

▶

◀

▶

Back

Close

Full Screen / Esc

Printer-friendly Version

Interactive Discussion



## 3.2 Resampling

To estimate quantiles of the distributions of extreme precipitation amounts, 3000-yr synthetic sequences of daily precipitation and temperature were generated by resampling from the 35-yr record of historical observations. These series were then transformed to future time series with the delta method described in Sects. 3.1.1 and 3.1.3. The method of time-series resampling of meteorological variables in the Rhine basin has been originally developed as part of a new methodology to determine the design discharge for flood protection in the Netherlands (Beersma and Buishand, 2003; Wójcik et al., 2000). Leander and Buishand (2007) and Leander et al. (2008) applied the same methodology for the first time to RCM data, but for the Meuse basin. Recently it has also been applied for the Rhine basin using time series from the RACMO RCM driven by the ECHAM5 GCM (Te Linde et al., 2010) and from an ensemble of RCMs in the Rheinblick2050 project (Görge et al., 2010).

Nearest-neighbour resampling is used to reproduce temporal correlation and to preserve the dependence between daily precipitation and temperature (Rajagopalan and Lall, 1999). In the multi-site application for the Rhine basin, the daily precipitation and temperature of the 134 HBV sub basins are sampled simultaneously with replacement from the historical data to preserve their mutual dependencies. Summary statistics of the daily precipitation and temperature fields are needed in this application to avoid problems with the high dimensional data space (Buishand and Brandsma, 2001).

To reduce the effect of seasonal variation, the search for nearest neighbours is restricted to days within a moving window of 61 days, centered on the calendar day of interest (Beersma, 2002; Wójcik et al., 2000). Further, the daily temperatures are standardized by subtracting the calendar-day mean and dividing by the calendar-day standard deviation before resampling. Daily precipitation is standardized by dividing by the mean wet-day precipitation amount of the calendar day of interest.

**HESSD**

9, 6533–6568, 2012

### Future changes in extreme precipitation in the Rhine basin

S. C. van Pelt et al.

Title Page

Abstract

Introduction

Conclusions

References

Tables

Figures

◀

▶

◀

▶

Back

Close

Full Screen / Esc

Printer-friendly Version

Interactive Discussion



## 4 Results

### 4.1 Change in mean, standard deviation and quantiles

Table 2 presents the changes in the 60 % and 90 % quantiles and the change in the mean excess after the transformation defined by Eqs. (1) and (11) has been applied to the 5-day sums of the observed precipitation series for the winter half-year (October–March) for all model simulations presented in Table 1. These changes were obtained by taking the median of the relative changes of the temporally smoothed estimates for each calendar month over the eight grid cells at the common GCM resolution and averaging these medians for the winter half-year, which is the main season of interest for high river discharge in the lower part of the Rhine basin. For the RCMs the transformation was applied after the RCM output was aggregated to the GCM grid resolution. In addition, the changes in the quantiles and the mean excess are shown for the bias corrected RCM output, again aggregated to the GCM grid. From Table 2 it can be seen that for the GCM simulations the changes in  $P_{90}$  and especially the mean excess ( $\bar{E}$ ) are generally stronger than the changes in the 60 % quantile, which supports the use of a non-linear delta method. In particular for GFDL2.1-CM2.1 and IPSL-CM4 the change in the mean excess largely exceeds the change in the 60 % and 90 % quantiles. In contrast, the relative changes in  $P_{60}$ ,  $P_{90}$  and mean excess are very similar for the RCM simulations. Also, the relative changes for the RCM output processed with the delta method are similar to those for the bias corrected RCM output. However, the relative changes for the RCMs generally differ from the relative changes of their driving GCM. The RCMs exhibit a smaller change in the mean excess ( $\bar{E}$ ) than their driving GCM, except those forced by ECHAM5r3.

For the remaining part of this study the results for the RCMs will refer to those obtained by the delta method, except when stated differently. In Table 3 changes in the mean and standard deviation for temperature and precipitation are shown. In winter the temperature change in the RCMs is almost equal to that in the GCMs. For summer,

## Future changes in extreme precipitation in the Rhine basin

S. C. van Pelt et al.

Title Page

Abstract

Introduction

Conclusions

References

Tables

Figures



Back

Close

Full Screen / Esc

Printer-friendly Version

Interactive Discussion



the change in the GCMs is a bit stronger, probably due to the fact that the RCMs have stronger orographic features, which especially in Alpine regions may have a systematic effect on the temperature change. The mean precipitation increases in winter and decreases in summer. For the GCM simulations the increase in the standard deviation of the 5-day precipitation sums is larger than the increase in the mean. This is consistent with the relatively large changes in the upper tail of the distribution ( $P_{90}, \bar{E}$ ) in these simulations. For both the GCM and RCM simulations the decrease in mean summer precipitation is accompanied by an increase in the standard deviation of the 5-day precipitation sums. The standard deviation of the daily temperatures decreases in winter and increases in summer. On average this means that in winter cold days warm more than warm days; in summer the opposite occurs. The increased temperature variability in winter and the decreased temperature variability in summer are consistent with other studies (Christensen et al., 2007; Kjellström et al., 2007), using different measures of daily temperature variability.

## 4.2 Precipitation extremes in short and long time series from the GCM-RCM ensemble

To assess the possible future change in the occurrence of extreme precipitation, the maximum 10-day basin-average precipitation amounts in the winter half-year from the transformed time series for future climate conditions are compared with those in the observed time series (Fig. 4). Both the ordered 10-day maxima from the original 35-yr time series and the resampled 3000-yr time series are shown. The spread between the future 10-day precipitation amounts is small at short return periods, but becomes larger at long return periods. For return periods longer than 10 yr, the spread for the resampled 3000-yr series is about 75 % of the spread for the original 35-yr series. For the 3000-yr series, the total ensemble spans a range between almost no change compared to the observations to an increase of about 30 % at the longest return periods.

## Future changes in extreme precipitation in the Rhine basin

S. C. van Pelt et al.

Title Page

Abstract

Introduction

Conclusions

References

Tables

Figures



Back

Close

Full Screen / Esc

Printer-friendly Version

Interactive Discussion



### 4.3 Range of return levels of maximum 10-day precipitation sums in the GCM and RCM ensemble

In Fig. 5 four return levels of the 10-day winter maximum basin-average precipitation for 2081–2100 are shown for all GCM and RCM simulations: the GCM and RCM ensembles that are created with the delta method and the bias corrected RCM simulations. The results are based on the 3000-yr resampled time series. The return levels were derived empirically from the ordered sample of the 10-day maxima. For the 1000-yr return level a distribution was fitted to the 15 largest values using an approach of Weisman (1978), because of the small number of exceedances of this return level (see also Appendix B). The estimated return level from the resampled observations is inserted in Fig. 5 as a reference representing current climate conditions. For the bias corrected RCM simulations, return levels for the future climate were obtained by multiplying the relative difference between the future and control simulation with this reference value.

For the 10-yr return level, the mean and spread in the GCM ensemble are comparable to those in the (delta method) RCM ensemble. For the 100-, 200- and 1000-yr return levels, the mean for the future period in the GCM ensemble is larger than the mean in the RCM ensemble. The spread within the GCM ensemble is slightly larger than the spread within the RCM ensemble for these return levels. This may be attributed to the larger size of the GCM ensemble (13 compared to five for the RCM ensemble). While the two RCM simulations that are forced by ECHAM5r3 show larger return levels of 10-day maximum basin-average precipitation than the driving GCM, all other RCM simulations show lower return levels than the GCM by which they are forced, in agreement with the changes in  $\bar{E}$  presented in Table 2. In particular for CLM the difference with the signal from the driving GCM is large for all return periods. For the RCM simulations, the results for the bias corrected model output are comparable to those generated with the delta method.

## Future changes in extreme precipitation in the Rhine basin

S. C. van Pelt et al.

Title Page

Abstract

Introduction

Conclusions

References

Tables

Figures



Back

Close

Full Screen / Esc

Printer-friendly Version

Interactive Discussion



## 5 Discussion and conclusions

This study explored the options to expand an existing range of RCM projections of changes in extreme multi-day precipitation in the Rhine basin, using an ensemble of GCM projections. The results of this study allow for a number of conclusions.

5 First, the selection of RCMs used in the Rheinblick2050 project does not appear to be strongly biased with respect to the multi-day extreme precipitation change imposed by the small ensemble of driving GCMs. As shown in Fig. 5, the small number of driving GCMs for the Rheinblick2050 RCM simulations covers the ranges deduced from the ensemble of 13 GCM simulations fairly well; the driving GCMs do not form a cluster  
10 or contain major outliers. When we look at the total ensemble we see that the ranges covered by the RCM simulations and the GCM simulations are similar. The ARPEGE-HIRHAM5 simulation, which was excluded in the present study, does not alter this result (see pp. 63, 64 of the Rheinblick2050 report; G6rger et al., 2010)

15 Second, for the RCM simulations the advanced non-linear delta method applied in this study generates a range of extreme multi-day precipitation changes that is similar to the range obtained directly from the bias corrected RCM simulations. This gives confidence in the application of the advanced non-linear delta method, using an ensemble of model projections. Responses derived from individual RCMs did show modest sensitivity to the selected method, but their ranking is similar for the two methods, which  
20 confirms our confidence in the delta method.

25 Third, the multi-day extreme precipitation signal deduced from the RCMs is not trivially related to the response derived from the driving GCMs. For three out of five RCM-GCM combinations, the RCM output leads to a smaller change of extreme 10-day precipitation sums than the corresponding GCM output. The two RCMs forced by ECHAM5r3 showed an increase in the change of the extreme 10-day precipitation sums, compared to the GCM output. Especially at long return periods, the individual paired GCM and RCM simulations show systematic differences. This could indicate that the RCMs have an influence on the signal of their driving GCMs, but the small

## Future changes in extreme precipitation in the Rhine basin

S. C. van Pelt et al.

Title Page

Abstract

Introduction

Conclusions

References

Tables

Figures



Back

Close

Full Screen / Esc

Printer-friendly Version

Interactive Discussion



number of simulations explored here does not permit a firm conclusion on the origin, nor robustness of this difference. Further research with larger ensembles and systematic exploration of potential causes is warranted. Possible causes of this response are locally generated natural variability (to be tested with larger ensembles), different physical expressions or parameterizations at higher spatial resolution, or dynamical/physical feedbacks that are represented differently by the driving GCM and the nested RCM.

The delta method applied in this study is useful as it is relatively cheap and it incorporates the observations. However, it has also some limitations. Since it is not physically but statistically based it potentially ignores relevant processes or feedbacks. The delta method as applied here neglects changes in the shape of the right tail of the distribution, by using a linear scaling of the excess above  $P_{90}$ . In addition the delta method required some subjective choices regarding temporal and spatial smoothing and bias correction of  $P_{60}$  and  $P_{90}$ . Most of these choices were tested carefully. As for other methods, the results of the delta method are influenced by sampling uncertainty resulting from the limited length of the observed and climate model time series, especially for long return periods.

For developing climate adaptation measures that deal with (future) flood risk, it is important to have knowledge about the changes in precipitation extremes. The results of this study provide an opportunity to base adaptation measures on an ensemble of 18 climate model simulations, which for current standards can be considered a large ensemble. The range of future changes in extreme multi-day precipitation, based on an ensemble of both GCMs and RCMs, gives more insight in the possible upper and lower bound of such changes, which is important information for water managers and flood risk studies (Ward et al., 2012). Figure 5 shows that using a sub-sample of GCM or RCM results alone could lead to an underestimation of the uncertainty range of future return levels, in particular for long return periods. Ideally, multi-model ensembles should therefore contain both RCM and GCM based results. However, as long as the RCMs and GCMs show different responses and the nature of these differences is unexplained, the authors recommend to present the responses for the different model ensembles

## Future changes in extreme precipitation in the Rhine basin

S. C. van Pelt et al.

[Title Page](#)[Abstract](#)[Introduction](#)[Conclusions](#)[References](#)[Tables](#)[Figures](#)[Back](#)[Close](#)[Full Screen / Esc](#)[Printer-friendly Version](#)[Interactive Discussion](#)

separately. This allows the user of this information to become aware that differences in the responses are (at least in part) related to differences in the type of climate model used.

## Appendix A

### 5 Relation between parameters in the transformation formula and extreme-value characteristics

In this appendix we relate the 90 % quantile  $P_{90}$  and the mean excess to properties of the distribution of seasonal maximum precipitation amounts. In the hydrological literature the generalized Pareto distribution (GP) has often been used to describe the distribution of the excesses of a high threshold  $u_0$  (e.g. Beguería, 2005; Van Montfort and Witter, 1986):

$$\Pr(P - u_0 \leq x | P > u_0) = \begin{cases} 1 - \left(1 + \frac{\kappa x}{\alpha_0}\right)^{-1/\kappa}, & \kappa \neq 0 \\ 1 - \exp\left(-\frac{x}{\alpha_0}\right), & \kappa = 0 \end{cases} \quad (\text{A1})$$

where  $\alpha_0$  is the scale parameter and  $\kappa$  the shape parameter. For  $\kappa = 0$  the GP distribution reduces to the exponential distribution. In our application  $P$  is the precipitation sum in an arbitrary 5-day interval. A reasonable assumption is that the consecutive 5-day values are independent. The number  $K_0$  of exceedances of  $u_0$  in a given season follows then a Poisson distribution with parameter  $\lambda_0$  (the mean number of exceedances) if  $u_0$  is sufficiently high. For the distribution of the seasonal maximum  $P_{\max}$  we then obtain:

$$H(x) = \Pr(P_{\max} \leq x) = \begin{cases} \exp\left\{-\left[1 + \xi\left(\frac{x-\mu}{\sigma}\right)\right]^{-1/\xi}\right\}, & \xi \neq 0 \\ \exp\left\{-\exp\left[-\left(\frac{x-\mu}{\sigma}\right)\right]\right\}, & \xi = 0 \end{cases} \quad (\text{A2})$$

20 which is a Generalized Extreme Value (GEV) distribution with location parameter  $\mu$ , scale parameter  $\sigma$ , and shape parameter  $\xi$ . The case  $\xi = 0$  is known as the Gumbel

## Future changes in extreme precipitation in the Rhine basin

S. C. van Pelt et al.

Title Page

Abstract

Introduction

Conclusions

References

Tables

Figures

◀

▶

◀

▶

Back

Close

Full Screen / Esc

Printer-friendly Version

Interactive Discussion



distribution. The three GEV distribution parameters are uniquely determined by the Poisson parameter  $\lambda_0$  and the GP distribution parameters  $\alpha_0$  and  $\kappa$  (Buishand, 1989; Wang, 1991):

$$\mu = \begin{cases} u_0 - \frac{\alpha_0}{\kappa} (1 - \lambda_0^\kappa), & \kappa \neq 0 \\ u_0 + \alpha_0 \ln(\lambda_0), & \kappa = 0 \end{cases}$$

$$\sigma = \alpha_0 \lambda_0^\kappa \quad (\text{A3})$$

$$\xi = \kappa$$

Note that Eq. (A2) only represents the distribution of the seasonal maxima for  $P_{\max} \geq u_0$ .

An important property of the GP distribution is that for all thresholds  $u > u_0$ , the excesses follow also a GP distribution with the same shape parameter  $\kappa$  but with a different scale parameter  $\alpha$  (e.g. Wang, 1991; Coles, 2001). The latter is related to the GEV scale parameter  $\sigma$  in the same way as  $\alpha_0$ :

$$\sigma = \alpha \lambda^\kappa \quad (\text{A4})$$

where  $\lambda$  is the mean number of exceedances of  $u$  in the season of interest. The mean of the excesses is given by (Coles, 2001):

$$\mu_E = \frac{\alpha}{1 - \kappa}, \quad \kappa < 1 \quad (\text{A5})$$

The GEV scale parameter gives the slope of the extreme-value plot of the seasonal maxima. From Eqs. (A4) and (A5), it follows:

$$\sigma = \lambda^\kappa (1 - \kappa) \mu_E, \quad \kappa < 1 \quad (\text{A6})$$

Hence, the GEV scale parameter is proportional to the mean excess. The constant of proportionality depends on the shape parameter. For  $\kappa = 0$ , we have  $\sigma = \mu_E$ . Because

## Future changes in extreme precipitation in the Rhine basin

S. C. van Pelt et al.

Title Page

Abstract

Introduction

Conclusions

References

Tables

Figures

◀

▶

◀

▶

Back

Close

Full Screen / Esc

Printer-friendly Version

Interactive Discussion



$\kappa$  generally does not differ much from zero for 5-day precipitation maxima, the constant of proportionality is close to 1.

If the excesses of the observed 5-day precipitation amounts follow a GP distribution, then the transformation (11) changes the scale parameter by a factor  $\overline{E^F}/\overline{E^C}$  and leaves the shape parameter unchanged. The slope of the extreme-value plot changes by the same factor. The transformation does, however, not make explicitly use of an underlying GP distribution. For instance, in the case of a Weibull distribution, it also changes the scale parameter by a factor  $\overline{E^F}/\overline{E^C}$  and leaves the shape parameter unchanged. A different transformation is needed to change the shape of the upper tail of the distribution of  $P$ . It is, however, difficult to find significant changes in the GP shape parameter.

Assuming independence of the 5-day precipitation sums, the number of exceedances of the 90 % quantile  $P_{90}$  in a season of  $5n$  days follows a binomial distribution with parameters  $n$  and  $p = 0.10$ . The probability that this quantile is not exceeded in a 90-day season is then  $0.9^{18} = 0.150$ . For a 180-day season this probability equals  $0.9^{36} = 0.023$  and thus  $P_{90}$  is in the extreme left tail of the distribution of  $P_{\max}$ . The delta method was also tested using the 95 % quantile  $P_{95}$  instead of  $P_{90}$ . The changes in the mean excesses of  $P_{95}$  turned out to be very sensitive to the method used to estimate  $P_{95}$  from the ordered sample of non-overlapping 5-day precipitation amounts owing to the small number of exceedances of this quantile in the short time-series used in this study. This sensitivity can be mitigated by taking all possible, overlapping 5-day precipitation amounts into account for estimating  $P_{95}$ .

**Future changes in extreme precipitation in the Rhine basin**

S. C. van Pelt et al.

Title Page

Abstract Introduction

Conclusions References

Tables Figures

◀ ▶

◀ ▶

Back Close

Full Screen / Esc

Printer-friendly Version

Interactive Discussion



## Appendix B

### Weissman approach for extreme values

The 1000-yr return values and their changes were estimated from the 15 largest values using the Weissman (1978) approach. Let  $X_{1n} \geq X_{2n} \geq \dots \geq X_{kn}$  be the  $k$  largest values in a sample of size  $n$  from a distribution  $F$ . In this study  $F$  refers to the distribution of the 10-day maximum basin – average precipitation in the winter half-year.

Under certain conditions on  $F$ , the joint density of  $X_{1n}, X_{2n}, \dots, X_{kn}$ , can for large  $n$  be approximated as (Weissman, 1978):

$$f_{1,\dots,k}(x_1, \dots, x_k) = \sigma^{-k} \exp \left[ -e^{-(x_k - \mu)/\sigma} - \sum_{i=1}^k (x_i - \mu)/\sigma \right] \quad (\text{B1})$$

where  $\mu$  is a location parameter (which depends on  $n$ ) and  $\sigma$  is a scale parameter. Equation (B1) applies if, after appropriate scaling, the distribution of the maximum  $X_{1n}$  tends to the Gumbel distribution as  $n \rightarrow \infty$ .

Maximization of the density  $f_{1,\dots,k}$  with respect to  $\mu$  and  $\sigma$  yields the maximum likelihood estimates:

$$\hat{\sigma} = \overline{X}_{kn} - X_{kn} \quad (\text{B2})$$

$$\hat{\mu} = X_{kn} + \hat{\sigma} \ln k \quad (\text{B3})$$

where  $\overline{X}_{kn}$  is the average of the  $k$  largest values. The  $T$ -year return value  $x_T$  is then estimated as:

$$\hat{x}_T = X_{kn} + \hat{\sigma} \ln(kT/n) \quad (\text{B4})$$

In this study:  $T = 1000$ ,  $n = 3000$  and  $k = 15$ .

## Future changes in extreme precipitation in the Rhine basin

S. C. van Pelt et al.

Title Page

Abstract

Introduction

Conclusions

References

Tables

Figures

◀

▶

◀

▶

Back

Close

Full Screen / Esc

Printer-friendly Version

Interactive Discussion



*Acknowledgements.* This research was carried out in the framework of the Dutch National Research Programme “Climate changes Spatial Planning”, as part of the project “Attention for Safety 2” and in the framework of the Dutch National Research Programme “Knowledge for Climate”. We thank Philip Ward, Jeroen Aerts and Otto de Keizer for their participation in the project and discussion on the methods, and Geert Jan van Oldenborgh for his comments on an earlier version of the manuscript.

## References

- Arnell, N. W. and Reynard, N. S.: The effects of climate change due to global warming on river flows in Great Britain, *J. Hydrol.*, 183, 397–424, 1996.
- 10 Beersma, J. J.: Rainfall generator for the Rhine basin: Description of 1000-year simulations, Royal Netherlands Meteorological Institute (KNMI), De Bilt, Publication 186-V, 18 pp., 2002.
- Beersma, J. J. and Buishand, T. A.: Multi-site simulation of daily precipitation and temperature conditional on the atmospheric circulation, *Clim. Res.*, 25, 121–133, 2003.
- Beguéría, S.: Uncertainties in partial duration series modelling of extremes related to the choice of the threshold value, *J. Hydrol.*, 303, 215–230, 2005.
- 15 Belz, J., Brahmer, G., Buiteveld, H., Engel, H., Grabher, R., Hodel, H., Krahe, P., Lammersen, R., Larina, M., Mendel, H.-G., Meuser, A., Müller, G., Plonka, B., Pfister, L., and Vuuren, W. V.: Das Abflussregime des Rheins und seiner Nebenflüsse im 20. Jahrhundert: Analyse, Veränderungen, Trends, International Commission for Hydrology of the Rhine basin (CHR), Lelystad, The Netherlands, Report no. I-22, 377 pp., 2007.
- 20 Beniston, M., Stephenson, D., Christensen, O., Ferro, C., Frei, C., Goyette, S., Halsnaes, K., Holt, T., Jylhä, K., and Koffi, B.: Future extreme events in European climate: An exploration of regional climate model projections, *Climatic Change*, 81, 71–95, 2007.
- Bernstein, L., Bosch, P., Canziani, O., Chen, Z., Christ, R., Davidson, O., Hare, W., Huq, S., Karoly, D., Kattsov, V., Kundzewicz, Z., Liu, J., Lohman, U., Mannin, M., Matsuno, T., Mene, B., Metz, B., Mirza, M., Nicholls, N., Nurse, L., Pachauri, R., Palutikof, J., Parry, M., Qin, D., Ravindranath, N., Reisinger, A., Ren, J., Riahi, K., Rosenzweig, C., Rusticucci, M., Schneider, S., Sokona, Y., Solomon, S., Stott, P., Stouffer, R., Sugiyama, T., Swart, R., Tirpak, D., Vogel, C., and Yohe, G.: Climate change 2007: Synthesis report, Intergovernmental Panel on Climate Change (IPCC), Geneva, 1–52, 2007.
- 30

## Future changes in extreme precipitation in the Rhine basin

S. C. van Pelt et al.

Title Page

Abstract

Introduction

Conclusions

References

Tables

Figures



Back

Close

Full Screen / Esc

Printer-friendly Version

Interactive Discussion



- Buishand, T. A.: Statistics of extremes in climatology, *Stat. Neerl.*, 43, 1–30, 1989.
- Buishand, T. A. and Brandsma, T.: Multisite simulation of daily precipitation and temperature in the Rhine basin by nearest-neighbor resampling, *Water Resour. Res.*, 37, 2761–2776, doi:10.1029/2001wr000291, 2001.
- 5 Buonomo, E., Jones, R., Huntingford, C., and Hannaford, J.: On the robustness of changes in extreme precipitation over Europe from two high resolution climate change simulations, *Q. J. Roy. Meteor. Soc.*, 133, 65–81, doi:10.1002/qj.13, 2007.
- Christensen, J. H., Hewitson, B., Busuioc, A., Chen, A., Gao, X., Held, I., Jones, R., Kolli, R. K., Kwon, W. T., Laprise, R., Magaña Rueda, V., Mearns, L., Menéndez, C. G., Räisänen, J., Rinke, A., Sarr, A., and Whetton, P.: Regional climate projections in: *Climate change 2007: The physical science basis. Contribution of working group I to the fourth assessment report of the Intergovernmental Panel on Climate Change*, United Kingdom and New York, NY, USA, 847–940, 2007.
- 10 Coles, S.: *An introduction to statistical modeling of extreme values*, Springer Verlag, Londen, UK, 2001.
- 15 Delworth, T. L., Broccoli, A. J., Rosati, A., Stouffer, R. J., Balaji, V., Beesley, J. A., Cooke, W. F., Dixon, K. W., Dunne, J., and Dunne, K.: GFDL's CM2 global coupled climate models. Part I: Formulation and simulation characteristics, *J. Climate*, 19, 643–674, 2006.
- Díaz-Nieto, J. and Wilby, R. L.: A comparison of statistical downscaling and climate change factor methods: Impacts on low flows in the river Thames, United Kingdom, *Climatic Change*, 20 69, 245–268, 2005.
- Disse, M. and Engel, H.: Flood events in the Rhine basin: Genesis, influences and mitigation, *Nat. Hazards*, 23, 271–290, doi:10.1023/a:1011142402374, 2001.
- Flato, G.: The third generation coupled global climate model (CGCM3), Canadian Centre for Climate Modelling and Analysis: Canada, available at: <http://www.ec.gc.ca/ccmac-cccma/default.asp?lang=En&n=1299529F-1> (last access: 24 May 2012), 2005.
- 25 Fowler, H. J. and Ekström, M.: Multi-model ensemble estimates of climate change impacts on UK seasonal precipitation extremes, *Int. J. Climatol.*, 29, 385–416, doi:10.1002/joc.1827, 2009.
- 30 Fowler, H. J., Blenkinsop, S., and Tebaldi, C.: Linking climate change modelling to impacts studies: Recent advances in downscaling techniques for hydrological modelling, *Int. J. Climatol.*, 27, 1547–1578, 2007.

---

**Future changes in extreme precipitation in the Rhine basin**S. C. van Pelt et al.

---

Title Page

Abstract

Introduction

Conclusions

References

Tables

Figures

◀

▶

◀

▶

Back

Close

Full Screen / Esc

Printer-friendly Version

Interactive Discussion



---

**Future changes in extreme precipitation in the Rhine basin**S. C. van Pelt et al.

---

[Title Page](#)[Abstract](#)[Introduction](#)[Conclusions](#)[References](#)[Tables](#)[Figures](#)[◀](#)[▶](#)[◀](#)[▶](#)[Back](#)[Close](#)[Full Screen / Esc](#)[Printer-friendly Version](#)[Interactive Discussion](#)

- Frei, C., Schöll, R., Fukutome, S., Schmidli, J., and Vidale, P. L.: Future change of precipitation extremes in Europe: Intercomparison of scenarios from regional climate models, *J. Geophys. Res.*, 111, D06105, doi:10.1029/2005jd005965, 2006.
- 5 Gordon, C., Cooper, C., Senior, C. A., Banks, H., Gregory, J. M., Johns, T. C., Mitchell, J. F. B., and Wood, R. A.: The simulation of SST, sea ice extents and ocean heat transports in a version of the Hadley Centre coupled model without flux adjustments, *Clim. Dynam.*, 16, 147–168, doi:10.1007/s003820050010, 2000.
- Gordon, H., Rotstayn, L., McGregor, J., Dix, M., Kowalczyk, E., O'Farrell, S., Waterman, L., Hirst, A., Wilson, S., and Collier, M.: The CSIRO Mk3 climate system model, CSIRO Atmospheric Research, Aspendale, Australia, Technical Paper no. 60, 134 pp., 2002.
- 10 Görgen, K., Beersma, J., Brahmer, G., Buiteveld, H., Carambia, M., de Keizer, O., Krahe, P., Nilson, E., Lammersen, R., Perrin, C., and Volken, D.: Assessment of climate change impacts on discharge in the Rhine river basin: Results of the RheinBlick2050 project, International Commission for the Hydrology of the Rhine basin (CHR), Lelystad, Report no. I-23, 229 pp., 2010.
- 15 Graham, L., Hagemann, S., Jaun, S., and Beniston, M.: On interpreting hydrological change from regional climate models, *Climatic Change*, 81, 97–122, 2007.
- Hanel, M. and Buishand, T.: Analysis of precipitation extremes in an ensemble of transient regional climate model simulations for the Rhine basin, *Clim. Dynam.*, 36, 1135–1153, doi:10.1007/s00382-010-0822-2, 2011.
- 20 Hasumi, H. and Emori, S.: K-1 coupled model (MIROC) description, Center for Climate System Research, University of Tokyo, Tokyo, K-1 Technical Report, 34 pp., 2004.
- Jacob, D.: A note to the simulation of the annual and inter-annual variability of the water budget over the Baltic Sea drainage basin, *Meteorol. Atmos. Phys.*, 77, 61–73, 2001.
- 25 Jones, R.: Generating high resolution climate change scenarios using PRECIS, Met Office, Hadley Centre, Exeter, UK, 35 pp., 2004.
- Kendon, E. J., Jones, R. G., Kjellström, E., and Murphy, J. M.: Using and designing GCM-RCM ensemble regional climate projections, *J. Climate*, 23, 6485–6503, doi:10.1175/2010JCLI3502.1, 2010.
- 30 Kjellström, E., Bärring, L., Jacob, D., Jones, R., Lenderink, G., and Schär, C.: Modelling daily temperature extremes: Recent climate and future changes over Europe, *Climatic Change*, 81, 249–265, 2007.

## Future changes in extreme precipitation in the Rhine basin

S. C. van Pelt et al.

Title Page

Abstract

Introduction

Conclusions

References

Tables

Figures

◀

▶

◀

▶

Back

Close

Full Screen / Esc

Printer-friendly Version

Interactive Discussion



- Klemeš, V.: Tall tales about tails of hydrological distributions I, *J. Hydrol. Eng.*, 5, 227–231, 2000a.
- Klemeš, V.: Tall tales about tails of hydrological distributions II, *J. Hydrol. Eng.*, 5, 232–239, 2000b.
- 5 Kyselý, J. and Beranová, R.: Climate-change effects on extreme precipitation in central Europe: Uncertainties of scenarios based on regional climate models, *Theor. Appl. Climatol.*, 95, 361–374, doi:10.1007/s00704-008-0014-8, 2009.
- Kyselý, J., Gaál, L., Beranová, R., and Plavcová, E.: Climate change scenarios of precipitation extremes in central Europe from ensembles regional climate models, *Theor. Appl. Climatol.*, 104, 529–542, doi:10.1007/s00704-010-0362-z, 2011.
- 10 Leander, R. and Buishand, T. A.: Resampling of regional climate model output for the simulation of extreme river flows, *J. Hydrol.*, 332, 487–496, 2007.
- Lenderink, G., Van den Hurk, B., Van Meijgaard, E., Van Ulden, A., and Cuijpers, H.: Simulation of present-day climate in RACMO2: First results and model developments, Royal Netherlands Meteorological Institute (KNMI), De Bilt, Technical Report no. TR-252, 24 pp., 2003.
- 15 Lenderink, G., Buishand, A., and van Deursen, W.: Estimates of future discharges of the river Rhine using two scenario methodologies: direct versus delta approach, *Hydrol. Earth Syst. Sci.*, 11, 1145–1159, doi:10.5194/hess-11-1145-2007, 2007.
- 20 Marti, O., Braconnot, P., Bellier, J., Benshila, R., Bony, S., Brockmann, P., Cadule, P., Caubel, A., Denvil, S., Dufresne, J., Fairhead, L., Filiberti, M. A., Fichefet, T., Foujols, M. A., Friedlingstein, P., Grandpeix, J. Y., Hourdin, F., Krinner, G., Lévy, C., Madec, G., Musat, L., De Noblet, M., Polcher, J., and Talandier, C.: The new IPSL climate system model: Ipslcm4 Inst. Pierre Simon Laplace des Sciences de l'Environnement Global, Paris, Case 101, 86 pp., 2006.
- 25 Meehl, G., Covey, C., Delworth, T. L., and Latif, M.: The WCRP CMIP3 multi-model dataset: A new era in climate change research, *B. Am. Meteorol. Soc.*, 88, 1383–1394, 2007.
- Menzel, L., Thieken, A., Schwandt, D., and Bürger, G.: Impact of climate change on the regional hydrology-scenario-based modelling studies in the German Rhine catchment, *Nat. Hazards*, 38, 45–61, 2006.
- 30 Min, S., Legutke, S., Hense, A., and Kwon, W.: Internal variability in a 1000-year control simulation with the coupled climate model ECHO-G-I. Near-surface temperature, precipitation and mean sea level pressure, *Tellus A*, 57, 605–621, doi:10.1111/j.1600-0870.2005.00133.x, 2005.

## Future changes in extreme precipitation in the Rhine basin

S. C. van Pelt et al.

Title Page

Abstract

Introduction

Conclusions

References

Tables

Figures

◀

▶

◀

▶

Back

Close

Full Screen / Esc

Printer-friendly Version

Interactive Discussion



Nikulin, G., Kjellström, E., Hansson, U. L. F., Strandberg, G., and Ullerstig, A.: Evaluation and future projections of temperature, precipitation and wind extremes over Europe in an ensemble of regional climate simulations, *Tellus A*, 63, 41–55, doi:10.1111/j.1600-0870.2010.00466.x, 2011.

5 Photiadou, C. S., Weerts, A. H., and van den Hurk, B. J. J. M.: Evaluation of two precipitation data sets for the Rhine River using streamflow simulations, *Hydrol. Earth Syst. Sci.*, 15, 3355–3366, doi:10.5194/hess-15-3355-2011, 2011.

Prudhomme, C. and Davies, H.: Assessing uncertainties in climate change impact analyses on the river flow regimes in the UK Part 2: Future climate, *Climatic Change*, 93, 197–222, 2009.

10 Prudhomme, C., Reynard, N., and Crooks, S.: Downscaling of global climate models for flood frequency analysis: Where are we now?, *Hydrol. Process.*, 16, 1137–1150, doi:10.1002/hyp.1054, 2002.

Rajagopalan, B. and Lall, U.: A  $k$ -nearest-neighbor simulator for daily precipitation and other weather variables, *Water Resour. Res.*, 35, 3089–3101, 1999.

15 Roeckner, E., Bäuml, G., Bonaventura, L., Brokopf, R., Esch, M., Giorgetta, M., Hagemann, S., Kirchner, I., Kornblueh, L., Manzini, E., Rhodin, A., Schlese, U., Schulzweida, U., and Tompkins, A.: The atmospheric general circulation model ECHAM5. Part I: Model description, Max Planck Institute for Meteorology Hamburg, Report no. 218, 127 pp., 2003.

Rowell, D. P.: A demonstration of the uncertainty in projections of UK climate change resulting from regional model formulation, *Climatic Change*, 79, 243–257, 2006.

20 Salas-Méla, D., Chauvin, F., Déqué, M., Douville, H., Gueremy, J., Marquet, P., Planton, S., Royer, J., and Tyteca, S.: Description and validation of the CNRM-CM3 global coupled model, Centre National de Recherches Météorologiques (CNRM), Météo France, Toulouse, 2005.

25 Steppeler, J., Doms, G., Schättler, U., Bitzer, H., Gassmann, A., Damrath, U., and Gregoric, G.: Meso-gamma scale forecasts using the nonhydrostatic model Im, *Meteorol. Atmos. Phys.*, 82, 75–96, 2003.

Te Linde, A. H., Aerts, J. C. J. H., Bakker, A. M. R., and Kwadijk, J. C. J.: Simulating low-probability peak discharges for the Rhine basin using resampled climate modeling data, *Water Resour. Res.*, 46, W03512, doi:10.1029/2009wr007707, 2010.

30 Ulbrich, U. and Fink, A.: The January 1995 flood in Germany: Meteorological versus hydrological causes, *Phys. Chem. Earth*, 20, 439–444, 1995.

## Future changes in extreme precipitation in the Rhine basin

S. C. van Pelt et al.

Title Page

Abstract

Introduction

Conclusions

References

Tables

Figures

◀

▶

◀

▶

Back

Close

Full Screen / Esc

Printer-friendly Version

Interactive Discussion



Van der Linden, P. and Mitchell, J.: Ensembles; climate change and its impacts: Summary of research and results from the ensembles project, Met Office Hadley Centre, Exeter, UK, 160 pp., 2009.

5 Van Montfort, M. and Witter, J.: The generalized pareto distribution applied to rainfall depths, Hydrolog. Sci. J., 31, 151–162, 1986.

Wang, Q.: The pot model described by the generalized pareto distribution with poisson arrival rate, J. Hydrol., 129, 263–280, 1991.

Ward, P. J., van Pelt, S. C., de Keizer, O., Aerts, J. C. J. H., and Beersma, J. J.: Probabilistic flood risk assessment, Journal of Flood Risk Management, in review, 2012.

10 Weissman, I.: Estimation of parameters and larger quantiles based on the  $k$  largest observations, J. Am. Stat. Assoc., 73, 812–815, 1978.

Wilby, R. L. and Harris, I.: A framework for assessing uncertainties in climate change impacts: Low-flow scenarios for the river Thames, UK, Water Resour. Res., 42, W02419, doi:10.1029/2005WR004065, 2006.

15 Wójcik, R., Beersma, J. J., and Buishand, T.: Rainfall generator for the Rhine basin. Multi-site generation of weather variables for the entire drainage area, Royal Netherlands Meteorological Institute (KNMI), De Bilt, 38 pp., 2000.

20 Yukimoto, S., Noda, A., Kitoh, A., Hosaka, M., Yoshimura, H., Uchiyama, T., Shibata, K., Arakawa, O., and Kusunoki, S.: Present-day climate and climate sensitivity in the meteorological research institute coupled GCM version 2.3 (MRI-CGCM2.3), J. Meteorol. Soc. Jpn., 84, 333–363, 186-V, 2006.

## Future changes in extreme precipitation in the Rhine basin

S. C. van Pelt et al.

**Table 1.** GCM and RCM simulations used in this study. Note that two different transient simulations with the ECHAM5 model (r1 and r3, which refer to runs with different initial conditions) were used as RCM boundary conditions; two RCMs are forced by ECHAM5r3.

GCM	RCM	GCM References	RCM References
CGCM3.1T63		Flato (2005)	
CNRM-CM3		Salas-Méla et al. (2005)	
CSIRO-Mk3.0		Gordon et al. (2002)	
ECHAM5r1	REMO_10	Roeckner et al. (2003)	Jacob (2001)
ECHAM5r3	RACMO		Lenderink (2003)
	REMO		Jacob (2001)
GFDL-CM2.0		Delworth et al. (2006)	
GFDL-CM2.1			
HADCM3Q0	CLM	Gordon et al. (2000)	Steppeler et al. (2003)
HADCM3Q3	HADRM3Q3		Jones (2004)
IPSL-CM4		Marti et al. (2006)	
MIROC3.2 hires		Hasumi and Emori (2004)	
MIUB		Min et al. (2005)	
MRI-CGCM2.3.2		Yukimoto et al. (2006)	

Title Page

Abstract

Introduction

Conclusions

References

Tables

Figures

◀

▶

◀

▶

Back

Close

Full Screen / Esc

Printer-friendly Version

Interactive Discussion



**Table 2.** Relative changes in the 60 % quantile, the 90 % quantile and mean excess ( $\bar{E}$ ) after a transformation of the 5-day precipitation sums of the observed precipitation based on the simulated changes of a GCM or RCM. The changes are basin-average relative changes for the winter half-year (October–March). The results in the columns headed  $P_{60}^{\text{DIR}}$ ,  $P_{90}^{\text{DIR}}$  and  $\bar{E}^{\text{DIR}}$  refer to the bias corrected RCM output, which are taken directly from the Rheinblick2050 project. The relative changes are based on the differences between the control and future period of the RCM.

GCM/RCM	$P_{60}$	$P_{90}$	$\bar{E}$	$P_{60}^{\text{DIR}}$	$P_{90}^{\text{DIR}}$	$\bar{E}^{\text{DIR}}$
CGCM3.1T63	1.10	1.11	1.22			
CNRM-CM3	0.97	1.04	1.28			
CSIRO-Mk3.0	1.01	1.05	1.17			
ECHAM5r1	0.98	1.04	1.25			
ECHAM5r1-REMO_10	1.11	1.10	1.00	1.12	1.08	1.07
ECHAM5r3	1.11	1.15	1.11			
ECHAM5r3-RACMO	1.18	1.19	1.21	1.21	1.22	1.19
ECHAM5r3-REMO	1.16	1.14	1.15	1.19	1.16	1.14
GFDL-CM2.0	1.04	1.11	1.21			
GFDL-CM2.1	1.05	1.10	1.41			
HADCM3Q0	1.12	1.17	1.35			
HADCM3Q0-CLM	1.03	1.10	1.07	1.02	1.12	1.04
HADCM3Q3	1.07	1.12	1.20			
HADCM3Q3-HADRM3	1.18	1.10	1.17	1.17	1.13	1.21
IPSL-CM4	0.89	1.01	1.36			
MIROC3.2	0.94	1.03	1.19			
MIUB	0.95	1.09	1.24			
MRI-CGCM2.3.2	1.05	1.09	1.34			
MEAN GCMs	1.02	1.08	1.26			
MEAN RCMs	1.13	1.13	1.12	1.14	1.14	1.13

**Future changes in extreme precipitation in the Rhine basin**

S. C. van Pelt et al.

Title Page

Abstract Introduction

Conclusions References

Tables Figures

◀ ▶

◀ ▶

Back Close

Full Screen / Esc

Printer-friendly Version

Interactive Discussion



## Future changes in extreme precipitation in the Rhine basin

S. C. van Pelt et al.

**Table 3.** Changes in the mean temperature and precipitation and in the standard deviation ( $\sigma$ ) of the daily temperatures and the 5-day precipitation sums after the transformation of the observations according to the changes in the GCM and RCM simulations. The changes are absolute (in  $^{\circ}\text{C}$ ) for mean temperature and relative for mean precipitation and the standard deviation. The changes are shown for the winter half-year (October–March) and the summer half-year (April–September).

	Temperature		Precipitation	
	Mean	$\sigma$	Mean	$\sigma$
Winter				
Mean GCMs	3.07	0.95	1.08	1.15
Mean RCMs	2.93	0.91	1.13	1.12
Summer				
Mean GCMs	3.58	1.10	0.88	1.02
Mean RCMs	2.90	1.06	0.91	1.06

[Title Page](#)
[Abstract](#)
[Introduction](#)
[Conclusions](#)
[References](#)
[Tables](#)
[Figures](#)
[Back](#)
[Close](#)
[Full Screen / Esc](#)
[Printer-friendly Version](#)
[Interactive Discussion](#)


## Future changes in extreme precipitation in the Rhine basin

S. C. van Pelt et al.

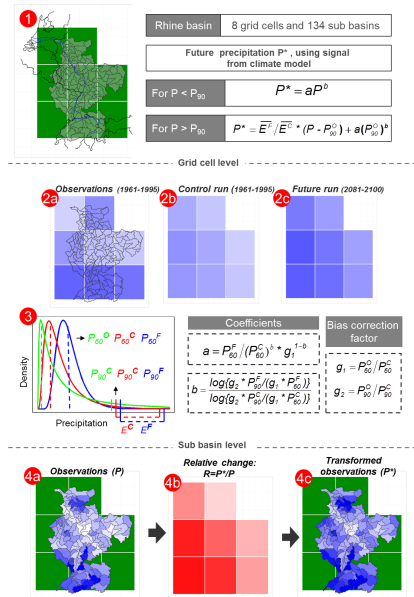


**Fig. 1.** Overview of the methodology. Panel 1 shows the Rhine basin, divided in 8 (GCM) grid cells and 134 sub-basins. Panel 2 shows the mean precipitation over a 5-day period in each grid cell for the observations and the control and future GCM simulation, all on grid cell level. The observations are upscaled to grid cell level by taking a weighted average over the sub-basins. In panel 3, the probability density of 5-day precipitation is shown, with the 60 % ( $P_{60}$ ) and the 90 % ( $P_{90}$ ) quantiles (for the observations as well as for GCM control and future simulations). Also the excess (the amount of precipitation > the 90 % quantile) is shown for the control and the future model run. Panel 4 displays the transformation. The daily observations in each sub-basin are multiplied by the change factor  $R$ , which is obtained from the observed ( $P$ ) and transformed ( $P^*$ ) 5-day precipitation amount and depends on the coefficients  $a$  and  $b$  and for  $P > P_{90}$  also on  $\bar{E}^F/\bar{E}^C$ . For each sub-basin the daily precipitation is transformed using the GCM signal from the grid cell that contains most of its surface area.

Title Page

Abstract Introduction

Conclusions References

Tables Figures

◀ ▶

◀ ▶

Back Close

Full Screen / Esc

Printer-friendly Version

Interactive Discussion

## Future changes in extreme precipitation in the Rhine basin

S. C. van Pelt et al.

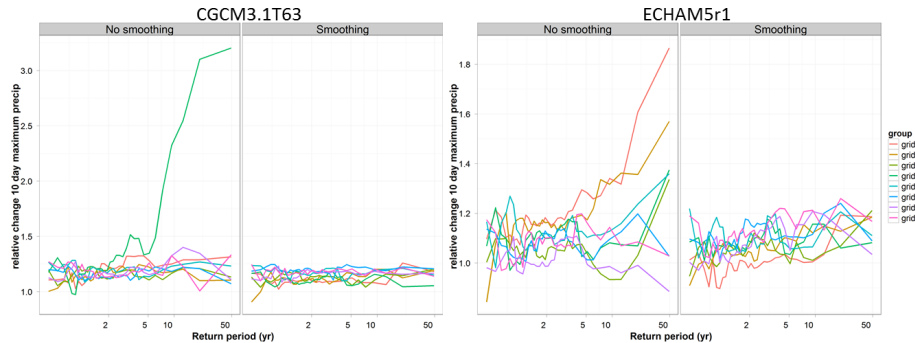


**Fig. 2.** Relative changes of the return levels of 10-day precipitation in the winter half-year (October–March) for each of the eight GCM grid cells covering the Rhine basin. Shown are results for the CGCM3.1T63 model simulation (left) and the ECHAM5r1 simulation (right). Within the figures for each model, the left panel shows the results for no temporal and spatial smoothing and the right panel shows the results with smoothing. Note, the difference in plotting scale for the CGCM3.1T63 and ECHAM5r1 results.

Title Page

Abstract

Introduction

Conclusions

References

Tables

Figures

◀

▶

◀

▶

Back

Close

Full Screen / Esc

Printer-friendly Version

Interactive Discussion



## Future changes in extreme precipitation in the Rhine basin

S. C. van Pelt et al.

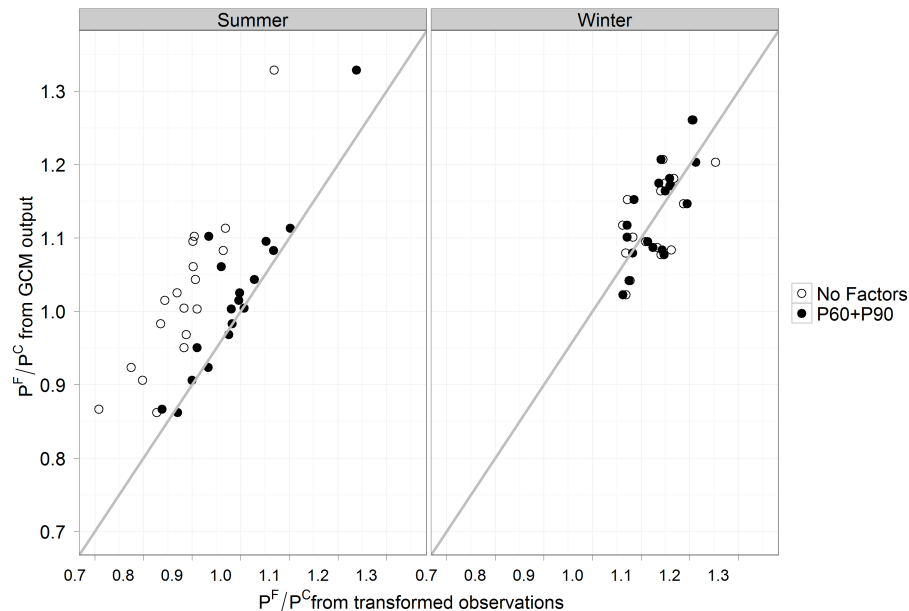


**Fig. 3.** Comparison of the relative change (future versus present day) of the mean 10-day maximum basin-average precipitation derived directly from the GCM simulations versus the change obtained from the transformation procedure for summer (left panel) and winter (right panel). The grey line is the 1:1 line. The results are shown for no bias correction (No Factors) and bias correction on  $P_{60}$  and  $P_{90}$  ( $P_{60} + P_{90}$ ).

[Title Page](#)
[Abstract](#)
[Introduction](#)
[Conclusions](#)
[References](#)
[Tables](#)
[Figures](#)
[◀](#)
[▶](#)
[◀](#)
[▶](#)
[Back](#)
[Close](#)
[Full Screen / Esc](#)
[Printer-friendly Version](#)
[Interactive Discussion](#)




## Future changes in extreme precipitation in the Rhine basin

S. C. van Pelt et al.

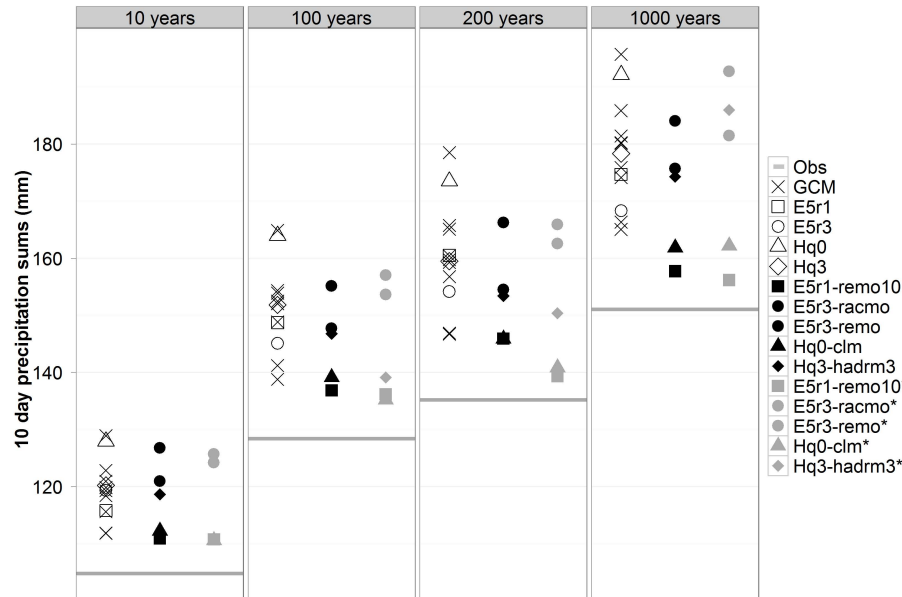


**Fig. 5.** Ranges of future 10-day basin-average precipitation for four return periods. The results are shown for the transformed observations based on the RCM and GCM ensembles and for the bias corrected RCM simulations. All GCM results are plotted in the first column of symbols. Open symbols represent GCM simulations that force at least one RCM, crosses refer to the results from the other GCM simulations. The second column represents transformed observations based on RCM simulations while the third column refers to the bias corrected RCM output. The RCMs are indicated by the same symbol as the driving GCM. The grey horizontal lines denote the return levels of the 10-day basin-average precipitation from the reference observations (i.e. the current climate).

Title Page

Abstract

Introduction

Conclusions

References

Tables

Figures

◀

▶

◀

▶

Back

Close

Full Screen / Esc

Printer-friendly Version

Interactive Discussion

